UC Davis
Mechanical and Aerospace Engineering

Title

Fundamental characteristics of flow past an array of hemispherical protrusions in millisecond microchannel reactors

Permalink

https://escholarship.org/uc/item/1363q7c9

Author

Chen, Junjie

Publication Date

2024-06-07

Supplemental Material

https://escholarship.org/uc/item/1363q7c9#supplemental

Fundamental characteristics of flow past an array of hemispherical protrusions in millisecond microchannel reactors

Junjie Chen [a, b,] *

[a] Department of Mechanical and Aerospace Engineering, College of Engineering, University of California, Davis, California, 95616, United States

[b] Department of Energy and Power Engineering, School of Mechanical and Power Engineering, Henan Polytechnic University, Jiaozuo, Henan, 454000, P.R. China

* Corresponding author, E-mail address: junjiem@tom.com

Abstract

Flow of a fluid past a body is a very complicated phenomenon. Computational fluid dynamics is used for studying the characteristics of flow past an array of hemispherical protrusions that is disposed on the wall surfaces of a millisecond microchannel reactor. Protrusions can be used to improve the transport processes involved, but the causes of the phenomena are still incompletely understood. Parametric analyses are performed under different sets of circumstances to delineate the role of geometric features and operation conditions in reactor performance. Dimensionless quantities are used to simplify the characterization of the reactor system with multiple interacting transport phenomena. The mechanisms involved in the intensified processes are analysed, and performance improvement recommendations are presented. The results indicate that the protruded reactor behaves effectively and good yields can be obtained with only milliseconds residence of the mixtures within the channels. The reactor offers the unique advantage for hydrogen production from methanol in that process intensification is realized while preserving the energy balance between the exothermic and endothermic processes. However, the flow rates must be adjusted as needed to maximize production of hydrogen and minimize pressure drops. The momentum diffusivity is more dominant around the protrusion regions than in the other regions. The thermal diffusivity is more dominant in the protruded channels than in the flat channels. The results have implications for hydrogen production and beyond for the study of transport phenomena in microchemical systems.

Keywords: Hemispherical protrusions; Fuel cells; Heat transfer; Microchannel reactors; Endothermic reactions; Mass transfer

1. Introduction

Historically, great strides have been made in manufacturing micro-electromechanical devices, thereby enabling microchemical systems to emerge more than three decades. Such systems have found wide applications due to improved heat and mass transfer [1, 2], and initial efforts focus upon the manipulation of selectivity [3], the remote handling and on-demand production of explosive and toxic chemicals [4], the high-throughput screening of catalysts and materials [5], and heat and mass transfer operations in chemical engineering [6]. Recently, there has been renewed interest in microchemical systems doe to their new applications, ranging from portable power generators [7] to heat sources [8]. The applications of heat sources have been noteworthy in fuel cells [8] due to their environmentally benign operation and high efficiency. Fuel cells are any of a class of devices that convert the chemical energy of a fuel directly into electricity by electrochemical reactions. A practical fuel cell is necessarily a complex system. It must have features to boost the activity of the fuel, pumps and blowers, fuel-storage containers, and a variety of sophisticated sensors and controls with which to monitor and

adjust the operation of the system. The operating capability and lifetime of each of these system design features may limit the performance of the fuel cell.

Fuel cells can convert the chemical energy of hydrogen, which is becoming an increasingly desired fuel, directly into electricity by electrochemical reactions. More particularly, proton-exchange membrane fuel cells are inherently high-efficiency devices and thus they are an increasingly attractive power supply for modern industry [9, 10]. However, a practical fuel cell is necessarily a complex system [11] and cost estimates are high for the total system [12]. High costs and limited success suppress interest in continuing developmental efforts. Fortunately, electrode and engineering design improvements may change these disadvantages [13, 14]. Widespread commercialization of proton-exchange membrane fuel cells depends upon economic competition with incumbent and advanced alternative technologies, represented by the ultimate cost target. The technology has been proven to be effective and workable, but attempts to make it commercially competitive are less successful, as such fabrication entails concerns with the high cost of platinum catalysts [15, 16], the relatively low energy density of hydrogen, the explosive power of hydrogen [17, 18], and especially the environmentally benign on-board and on-site production of hydrogen at the small scale.

The present study focuses upon the physics of heat and mass transfer processes in a protruded millisecond microchannel reactor, wherein a steam reforming reaction is proceeding and protrusions are used to improve the transport processes involved. Parametric analysis of the reactor system is carried out using a three-dimensional numerical model that is sufficiently detailed to delineate the role of geometric features and operation conditions in reactor performance. Computational fluid dynamics analyses are performed under different sets of circumstances. In analysing the mechanisms involved in the intensified processes, account is taken of the factors that may influence the reactor performance. New insights into the physics of the processes are presented, with recommendations on how to optimize reactor design for better performance. Dimensionless Prandtl numbers are used to indicate the ratio of momentum diffusivity to thermal diffusivity. The present study aims to understand the causes of the phenomena of process intensification in a protruded millisecond microchannel reactor. Particular emphasis is placed on delineating the role of geometric features and operation conditions in reactor performance. The results have implications for hydrogen production and beyond, for example, for the study of transport phenomena in microchannel reactors with a complicated structure.

2. Reactor model

2.1. Physical model

The present study relates to a process for steam reforming in a protruded millisecond microchannel reactor, wherein methanol and steam or water vapour are reacted to produce a hydrogen containing gas stream. Heat released by an oxidation process is typically required to drive the endothermic reforming reaction. The structure of the reactor utilized for producing hydrogen-rich gas is illustrated schematically by reference to Figure 1 with the coating and channel indicated. The design uses protrusions for the reforming channels to improve the transport processes involved. The inclusion of the protrusion arrays on the wall surfaces is motivated by great disparities in conversion and productivity between the flat and protruded channels, which will be discussed in detail later. However, there is not necessarily a need for the oxidation channels to use protrusions, as the chemical reaction proceeds rapidly. The protrusions are hemispherical in shape and arranged regularly on the wall surfaces to achieve the desired characteristics. The protrusions provide improvement by increasing the desirable disturbance of the flow over the washcoat coating surface where they are located [19, 20]. Another solution to the protrusions is to improve the transport characteristics by increasing the boundary area. Unfortunately, this may lead to the disadvantageous requirement for the protrusions in

the reactor wherein methanol is steam reformed, particularly since the design complexity does necessarily increase the capital and operation costs of hydrogen production. The potential solution of added protrusions to deal with enhanced heat and mass transfer considerations may disadvantageously complicate the flow process of the reactor, since a great loss of pressure may be encountered.
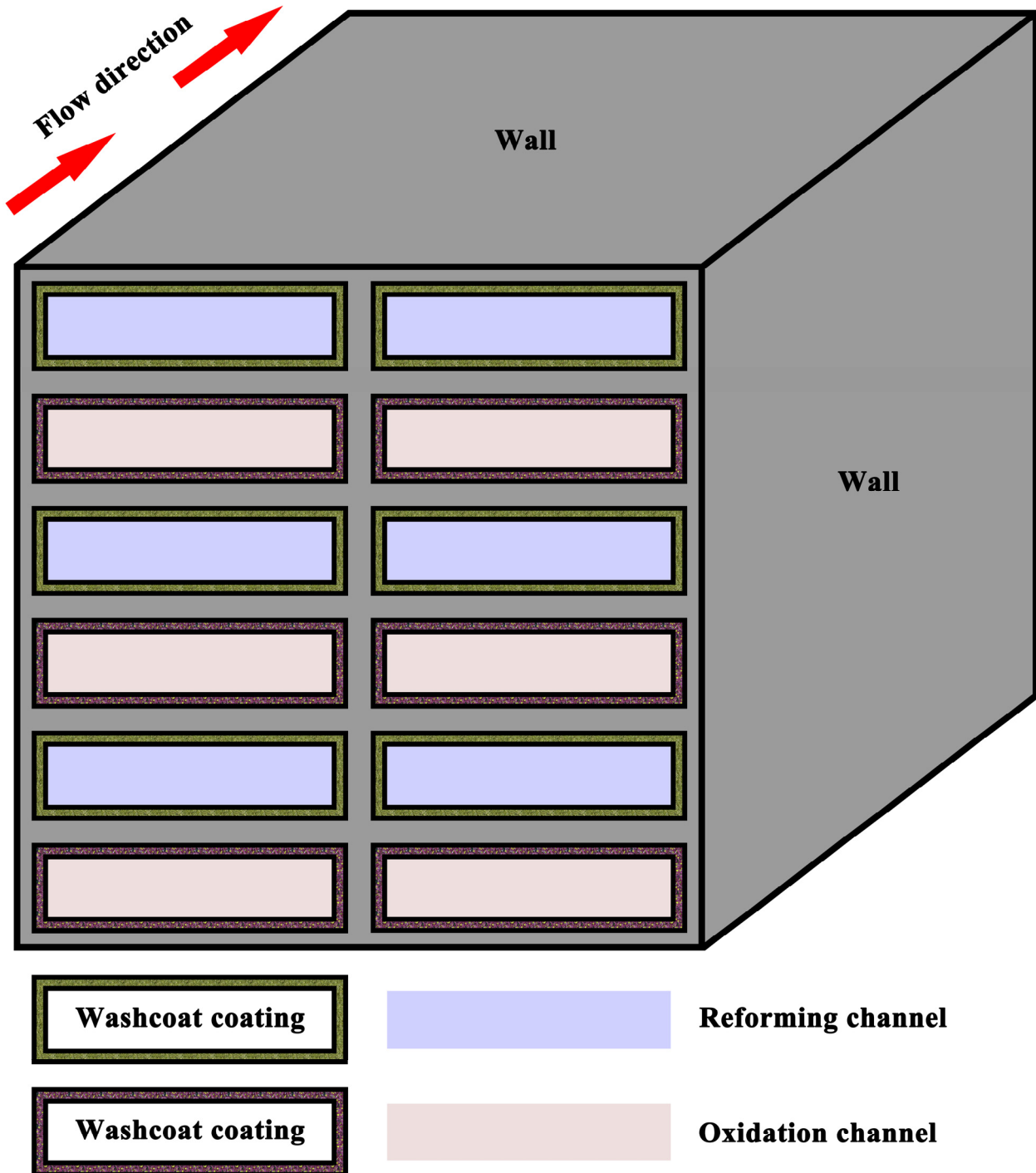

Figure 1. Illustration representation of the structure of the microchannel reactor for the production of a hydrogen containing gas stream by steam reforming with the coating and channel indicated.
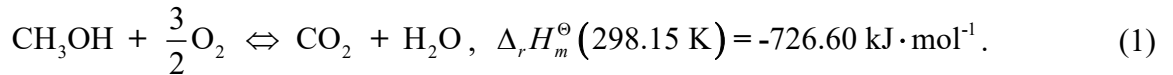
The stainless-steel walls of the channels are coated with catalyst washcoat compositions. The channels are rectangular in both cross section and longitudinal section. The reformation catalyst for converting methanol into hydrogen is a mixture of copper and zinc oxide supported on alumina. In addition, the oxidation catalyst is a mixture of copper oxide and zinc oxide supported on alumina. The channels are of uniform spacing along their length. The channels are 60.0 mm in length, 5.6 mm in

width, and 0.8 mm in height, the washcoat coatings are 0.20 mm in thickness, and the walls are 0.30 mm in thickness, unless otherwise expressly provided. For the feed stream to be reformed or oxidized, the gaseous reactant mixture is supplied to the reactor in a molar ratio of steam to methanol of 150:100 or with an equivalence ratio of methanol to air of 0.8, unless otherwise specified. The reactor operates at one atmosphere pressure with an inlet temperature of 100 °C for both the gaseous reactant mixtures. The gaseous reactant mixtures are introduced respectively into the reactor with a free-stream velocity of 1.2 m/s at the oxidation channel inlet and a free-stream velocity of 4.0 m/s at the reforming channel inlet, unless otherwise noted. At the free-stream velocities noted above, flow is laminar throughout the length of the channels. The feed compositions and inlet velocities can be adjusted, respectively, as needed to achieve the desired conversion level.
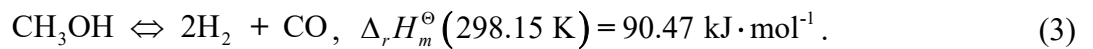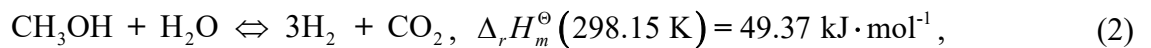
2.2. Chemical kinetics

Microchannel reactors have the inherent property that the reactions involved can occur at extremely high rates [21, 22]. Consequently, the reactor is designed to convert methanol in the vapour phase into hydrogen with only milliseconds residence of the mixture within the channels. There are a variety of chemical reactions that can occur in the reactor, including oxidation, reformation, decomposition, and water-gas shift reactions. Of especially critical importance in the analysis of the chemical processes are the amounts of heat released or required and the amounts of the products formed or reactants consumed, namely the rates of the reactions. There are many possible variations in detail, depending largely on the particular fuel that is used.

The catalytic oxidation reaction proceeds rapidly on the washcoat coating surface. The catalytic oxidation reaction is illustrated by the equation:

$$CH_3OH + \frac{3}{2}O_2 \Leftrightarrow CO_2 + H_2O, \quad \Delta_r H_m^\ominus (298.15\ \text{K}) = \text{-}726.60\ \text{kJ}\cdot\text{mol}^{-1}. \tag{1}$$

Note that here $\Delta_r H_m^\ominus$ is the heat of reaction in the standard state.

The steps of steam reforming to produce hydrogen are well known both economically and technically. More specifically, a hydrogen containing gas stream is produced in the reactor by the steam reforming and catalysed decomposition of methanol. The chemical equations for these reversible endothermic reactions are of the forms

$$CH_3OH + H_2O \Leftrightarrow 3H_2 + CO_2, \quad \Delta_r H_m^\ominus (298.15\ \text{K}) = 49.37\ \text{kJ}\cdot\text{mol}^{-1}, \tag{2}$$

$$CH_3OH \Leftrightarrow 2H_2 + CO, \quad \Delta_r H_m^\ominus (298.15\ \text{K}) = 90.47\ \text{kJ}\cdot\text{mol}^{-1}. \tag{3}$$

The reformed gas stream is subjected to a further process step, wherein carbon monoxide formed by the reformation and decomposition reactions is reacted with steam to produce carbon dioxide and hydrogen, as indicated by the following water-gas shift reaction

$$CO + H_2O \Leftrightarrow CO_2 + H_2, \quad \Delta_r H_m^\ominus (298.15\ \text{K}) = \text{-}41.10\ \text{kJ}\cdot\text{mol}^{-1}. \tag{4}$$
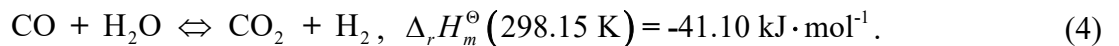
The kinetic model [23, 24] is used to account for the oxidation process. The kinetic model [25, 26] is used to account for the reformation, decomposition, and water-gas shift processes. The rates of the reactions can be expressed in the forms

$$r_O = 10^7 e^{-115000 R^{-1} T^{-1}} p_{CH_3OH}^{0.18} p_{O_2}^{0.18} p_{H_2O}^{-0.14}, \tag{5}$$

$$r_R = \left[k_R K_{CH_3O^{(\alpha)}}^{\vartheta} \left(p_{CH_3OH} p_{H_2}^{-0.5} \right) \left(1 - k_R^{-1} p_{H_2}^{3} p_{CO_2} p_{CH_3OH}^{-1} p_{H_2O}^{-1} \right) c_{S_\alpha}^{\pi} c_{S_{\alpha'}}^{\pi} \right]$$
$$\cdot \left[\left(1 + K_{CH_3O^{(\alpha)}}^{\vartheta} \left(p_{CH_3OH} p_{H_2}^{-0.5} \right) + K_{HCOO^{(\alpha)}}^{\vartheta} p_{CO_2} p_{H_2}^{0.5} + K_{OH^{(\alpha)}}^{\vartheta} \left(p_{H_2O} p_{H_2}^{-0.5} \right) \right) \left(1 + K_{H^{(\alpha')}}^{0.5} p_{H_2}^{0.5} \right) \right]^{-1}, \tag{6}$$

$$r_D = \left[k_D K_{CH_3O^{(\beta)}}^{\vartheta} \left(p_{CH_3OH} p_{H_2}^{-0.5} \right) \left(1 - k_D^{-1} p_{H_2}^2 p_{CO} p_{CH_3OH}^{-1} \right) c_{S_\beta}^{\pi} c_{S_{\beta'}}^{\pi} \right]$$
$$\cdot \left[\left(1 + K_{CH_3O^{(\beta)}}^{\vartheta} \left(p_{CH_3OH} p_{H_2}^{-0.5} \right) + K_{OH^{(\beta)}}^{\vartheta} \left(p_{H_2O} p_{H_2}^{-0.5} \right) \right) \left(1 + K_{H^{(\beta')}}^{0.5} p_{H_2}^{0.5} \right) \right]^{-1} , \tag{7}$$

$$r_W = \left[k_W^{\vartheta} K_{OH^{(\alpha)}}^{\vartheta} \left(p_{CO} p_{H_2O} p_{H_2}^{-0.5} \right) \left(1 - k_W^{-1} p_{H_2} p_{CO_2} p_{CO}^{-1} p_{H_2O}^{-1} \right) \left(c_{S_\alpha}^{\pi} \right)^2 \right]$$
$$\cdot \left[\left(1 + K_{CH_3O^{(\alpha)}}^{\vartheta} \left(p_{CH_3OH} p_{H_2}^{-0.5} \right) + K_{HCOO^{(\alpha)}}^{\vartheta} p_{CO_2} p_{H_2}^{0.5} + K_{OH^{(\alpha)}}^{\vartheta} \left(p_{H_2O} p_{H_2}^{-0.5} \right) \right) \right]^{-2} , \tag{8}$$

where r, p, k, K, c_S^{π}, and ϑ is the reaction rate, pressure, specific rate constant, chemical equilibrium constant, total concentration on the washcoat coating surface, and composite parameter, respectively, the subscripts α, α', β, and β' and the superscripts (α), (α'), (β), and (β') denote the active or adsorption sites, and the subscripts O, R, D, and W denote the oxidation, reformat! decomposition, and water-gas shift reactions, respectively.

3. Results and discussion

Performance comparisons are conducted between the reactors with flat and protruded reforming channels in terms of temperature, species mole fraction, and Prandtl number. The Prandtl number is defined as the ratio of momentum diffusivity to thermal diffusivity. The temperature, methanol mole fraction, and hydrogen mole fraction results are presented in Figure 2 with three-dimensional contour maps in the reactor with flat or protruded reforming channels. Accordingly, the carbon dioxide mole fraction and Prandtl number results are presented in Figure 3 with three-dimensional contour maps in the reactor with flat or protruded reforming channels. Methanol is oxidized rapidly in the reactor. The heat released by the oxidation reaction is supplied to the reactant mixture, since the reforming reaction is endothermic. The heat transfer has a dual effect: firstly, it does give rise to warming of the feed stream and secondly, it supplies the heat required for the reforming reaction. The protruded channels have a smaller methanol concentration and greater hydrogen and carbon dioxide concentrations at the reactor outlet than the flat channels. Flow of a fluid past a body is a very complicated phenomenon [27, 28]. For the case of protruded channels, wake vortices can be generated behind the protrusions [29, 30], which will create an almost stationary region of higher residence time and lower flow velocity and therefore of higher conversion. The protrusions provide further advantages in that the strength and rigidity of the wall can be enhanced, since the pressure differential across the wall may be relatively large. For the case of protruded channels, the reactant concentrations around the protrusion regions are lower than those in the other regions and the product concentrations around the protrusion regions are higher than those in the other regions due to the almost stationary regions created behind the protrusions. The ratio of the thickness of velocity to thermal boundary layer in laminar flow can be determined by use of the Prandtl number [31, 32]. The velocity and thermal boundary layers coincide with each other and momentum and thermal diffusion coefficients are comparable, if the Prandtl number is unity [31, 32]. Near the inlet end of the reactor, the thickness of velocity boundary layer in laminar flow is greater than the that of thermal boundary layer, as the Prandtl number is greater than unity. Near the outlet end of the reactor, the thickness of thermal boundary layer is greater than the that of velocity boundary layer, as the Prandtl number is less than unity. For the case of protruded channels, the fluid during flow past the protrusions has a Prandtl number greater than that during flow through the other regions, which means that the momentum diffusivity is more dominant around the protrusion regions than in the other regions. The fluid in the case of flow through the protruded channels has a Prandtl number less than that in the case of flow through the flat channels, which means that the thermal diffusivity is more dominant in the protruded channels than in the flat channels.
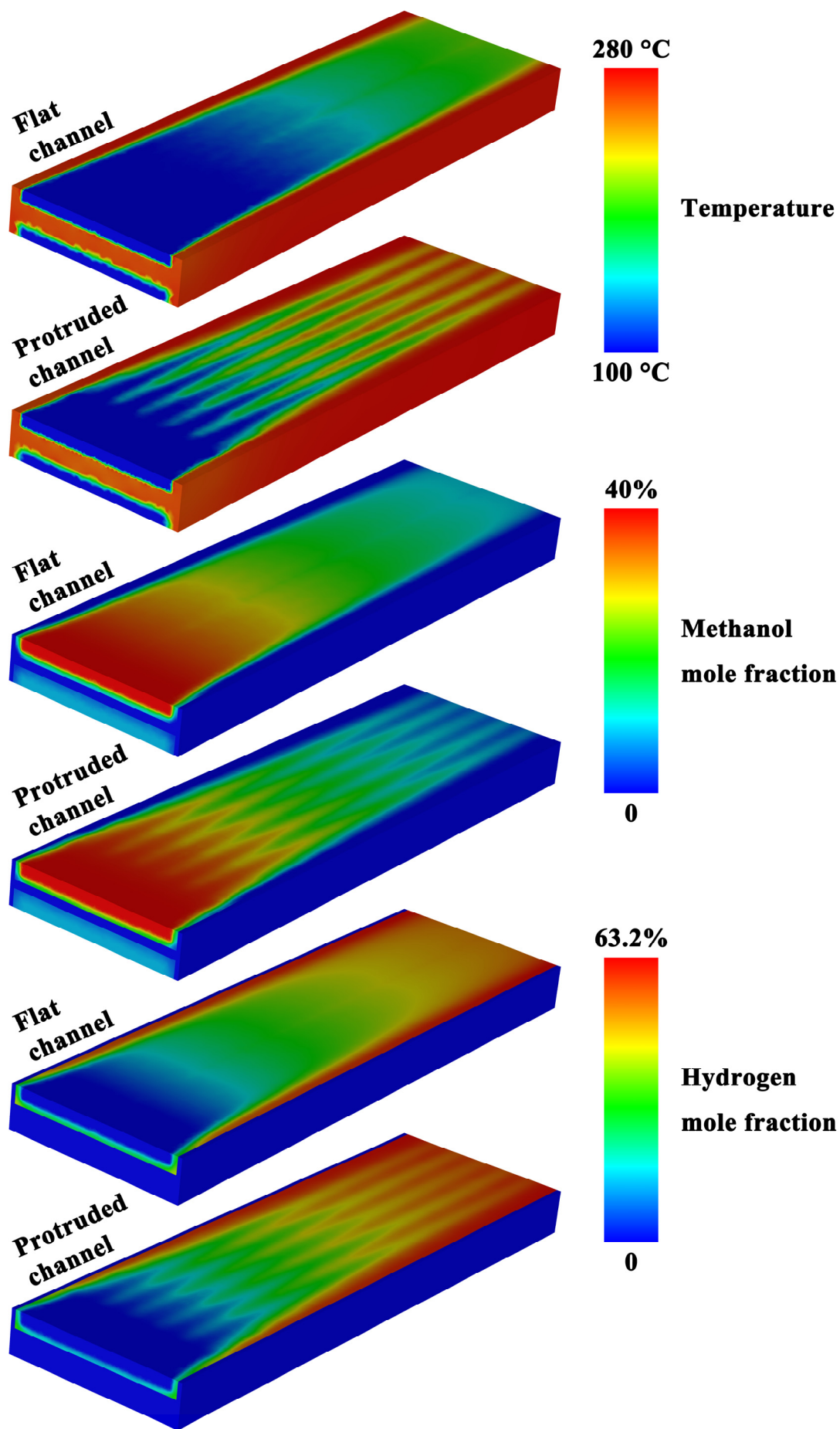
Figure 2. Three-dimensional contour maps of temperature, methanol mole fraction, and hydrogen mole fraction in the reactor with flat or protruded reforming channels.
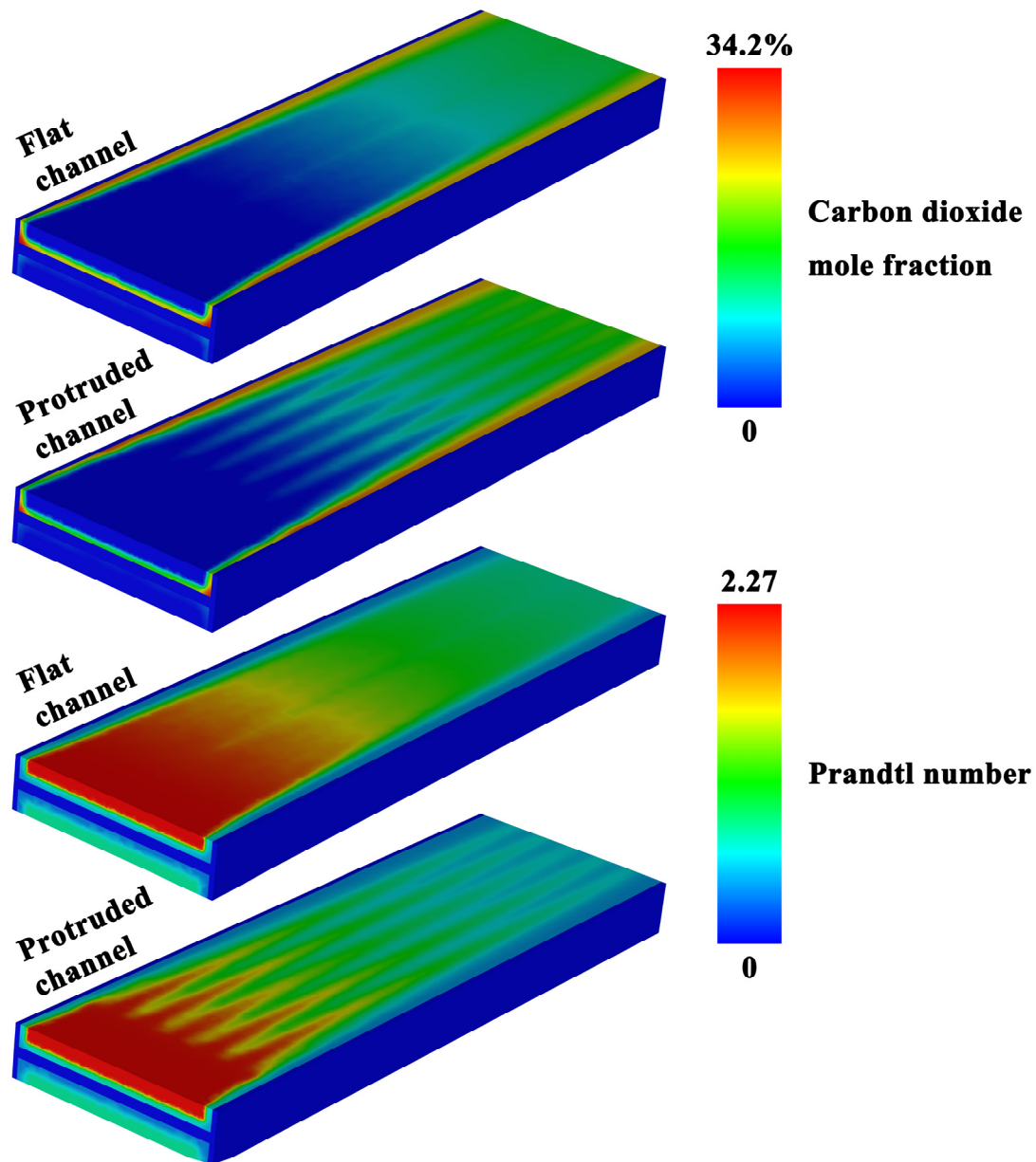
Figure 3. Three-dimensional contour maps of carbon dioxide mole fraction and Prandtl number in the reactor with flat or protruded reforming channels.

The laws of physical chemistry and physics govern the practicability and efficiency of chemical engineering operations. Energy changes, deriving from thermodynamic considerations, are particularly important. Mathematics is a basic tool in optimization and modelling. Optimization means arranging materials, facilities, and energy to yield as productive and economical an operation as possible. Modelling is the construction of theoretical mathematical prototypes of complex process systems.

The washcoat coating surface in the reactor is illustrated in Figure 4 with the spherical edge line and the spherical centre line indicated. The two-dimensional contour maps of temperature in a longitudinal section along the spherical edge or the spherical centre are illustrated in Figure 5 with the hemisphere location indicated, in which the washcoat coating surface in the reactor is illustrated schematically with the spherical edge line and the spherical centre line indicated. The two-dimensional contour maps of methanol mole fraction in a longitudinal section along the spherical edge or the spherical centre are illustrated in Figure 6 with the hemisphere location indicated. Steep gradients of temperature do exist in the reactor where the reaction is proceeding, and the region of the fluid is referred to as a thermal boundary layer in which heat is transferred at the washcoat coating surface purely by conduction. At the washcoat coating surface, the protruded channel inherently has a

stationary layer of the fluid through which the transferred heat must pass, which is referred to as a velocity boundary layer. The thermal or velocity boundary layer increases progressively in thickness, in the presence of a smooth flow [33, 34], for instance, for the flat channel. The boundary layer insulates the bulk fluid from the wall, and thus it is strictly necessary to keep the boundary layer as thin as possible [35, 36]. The protrusions can be properly positioned within the channels to interrupt the smooth flow of the fluid at appropriate intervals in a way that the thickness of boundary layer can be reduced effectively. However, the interruptions must be continued, as the boundary layer in laminar flow immediately begins to thicken again [33, 34]. Successive continuous interruptions are achieved in the flow of the fluid in the protruded channels. Accordingly, methanol can be converted effectively to hydrogen due to the successive continuous interruptions in the presence of hemispherical protrusions. The temperatures in the protruded millisecond microchannel reactor are sufficient for reforming duty. In particular, the temperatures of the protrusions are relatively high and thus the endothermic reforming reaction is favoured. Heat is transferred rapidly into the protruded channel due to its very small dimension in the normal direction, while the gradients of temperature in the spanwise direction remain sufficiently constant. Typically, a protrusion defines a trailing edge and a leading edge, respectively, and the flow separation of the methanol-steam mixture passing over the protrusion occurs at the trailing edge of the protrusion, therefore generating a wake vortex downstream of the trailing edge [37, 38]. The velocity of flow of the fluid flowing in the bulk stream around or surrounding the protrusion while the reaction is proceeding is much higher than the velocity of flow of the stream in the vortex region, which will create an almost stationary region of higher residence time and therefore of higher conversion. On the other hand, the protruded design of the reactor provides a flow passage for the fluid comprising a succession of flow passage chamber portions separated from each other by intervening protrusion portions of smaller cross section, and thus of smaller flow capacity, transverse to the flow direction. Accordingly, the fluid travels through the reforming channel at a higher velocity in the protrusion portions than in the chamber portions. The fluid velocity in the protrusion portions is sufficiently high so that the thickness of the boundary layer on the washcoat coating surface can be effectively reduced, thereby facilitating the heat and mass transfer within the reactor. Additionally, the fluid flows as wake vortices behind the protrusions [39, 40], thereby establishing wake interference flow [41, 42] and consequently enhancing the rates of heat and mass transfer [43, 44]. While heat and mass transfer problems may be minimised, adding the protrusions while maintaining a constant inlet velocity will inevitably lead to a loss of pressure.
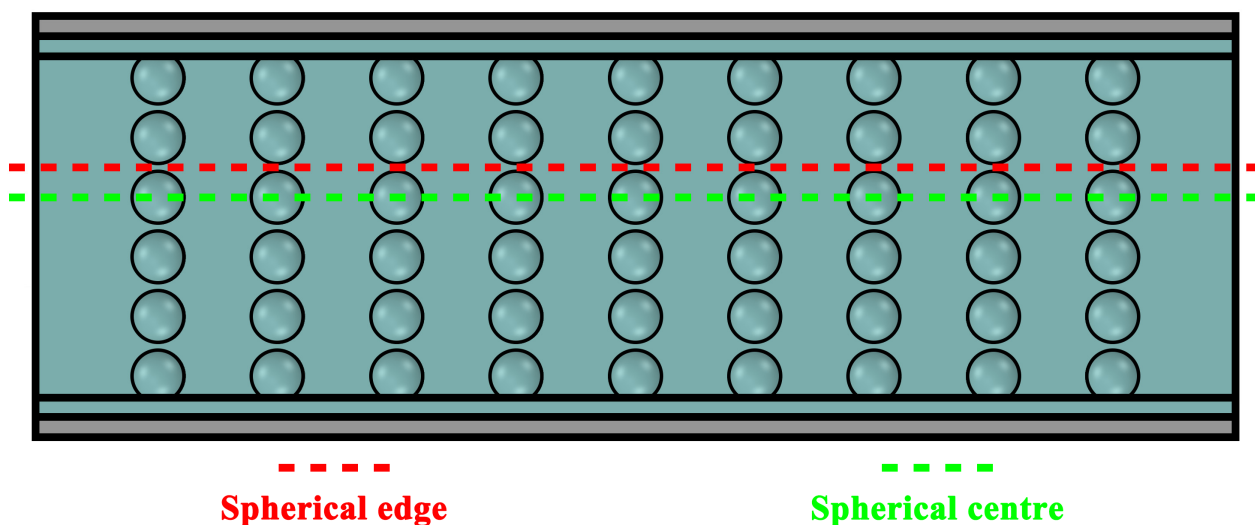

Figure 4. Illustration representation of the washcoat coating surface in the reactor with the spherical edge line and the spherical centre line indicated.

Temperature

280 °C

Longitudinal section along the spherical edge

Longitudinal section along the spherical centre
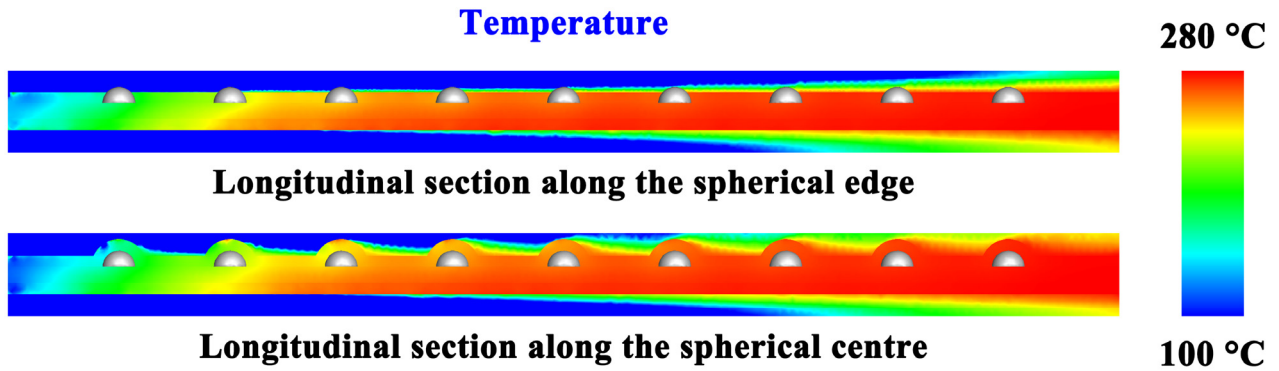
100 °C

Figure 5. Two-dimensional contour maps of temperature in a longitudinal section along the spherical edge or the spherical centre with the hemisphere location indicated.

Methanol mole fraction

40%

Longitudinal section along the spherical edge

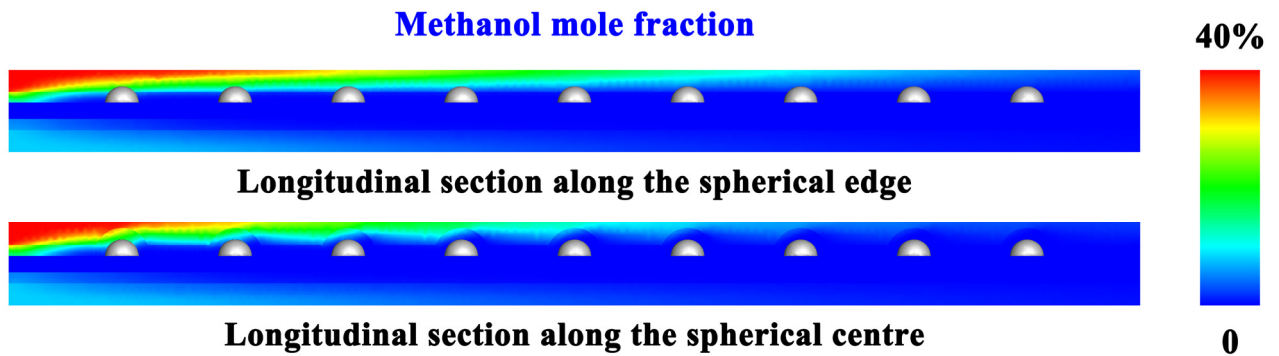**Longitudinal section along the spherical centre**

0

Figure 6. Two-dimensional contour maps of methanol mole fraction in a longitudinal section along the spherical edge or the spherical centre with the hemisphere location indicated.

Direct oxidation of fuels such as methanol in fuel cells at practical current densities with acceptable catalyst loadings is not as economically attractive as conversion of methanol fuel to a hydrogen-rich mixture of gases via steam reforming and subsequent electrochemical conversion of the hydrogen-rich fuel stream to direct current in the fuel cell [45, 46]. A very attractive fuel cell system currently undergoing commercial consideration is the reformed methanol fuel-phosphoric acid electrolyte-air system [47, 48]. The effect of the velocity at the reactor inlet on the methanol conversion and the hydrogen productivity is illustrated in Figure 7 in which the hydrogen productivity is calculated per channel. The conversion and productivity are sensitive to the velocity at the reactor inlet and the flowthrough structure of the channels. The protruded design of the reactor enables a higher conversion level and improved hydrogen productivity in the endothermic reforming process by virtue of improved species transport from and to the washcoat coating surface, since the fluid flows around the protrusions as wake vortices, as discussed above. Under the given operation conditions, the inlet velocity required for a given productivity level is lower than if no hemispherical protrusions are arranged. The low inlet velocity required for the required productivity level will lead to the relatively high conversion level achieved, even with the relatively short channels employed. Although lower inlet velocities can be utilized to achieve higher methanol conversion levels, relatively low hydrogen productivities may be unacceptable. At very high inlet velocities, the conversion to hydrogen is limited to relatively low levels, but the maximum productivity level can be achieved. This improved productivity may be especially important for the production of hydrogen-rich gas. The fluid travels smoothly or in regular paths, in contrast to turbulent flow, in which the fluid undergoes irregular fluctuations and mixing. In laminar flow, the velocity, pressure, and other flow properties at each point in the fluid remain constant. Laminar flow over a horizontal surface may be thought of as consisting of thin layers, or laminae, all parallel to each other. The fluid in contact with the horizontal surface is stationary, but all the other layers slide over each other. A perfect fluid, even while flowing, cannot sustain a tangential force; that

is, it lacks viscosity and is also referred to as an inviscid fluid. Some real fluids of low viscosity and heat conductivity approach this behaviour. Fluids of which the viscosity, or internal friction, must be taken into account are called viscous fluids and are further distinguished as Newtonian fluids if the viscosity is constant for different rates of shear and does not change with time. The viscosity of non-Newtonian fluids either varies with the rate of shear or varies with time, even though the rate of shear is constant. Fluids in a class in this last category that become thinner and less viscous as they continue to be stirred are called thixotropic fluids.
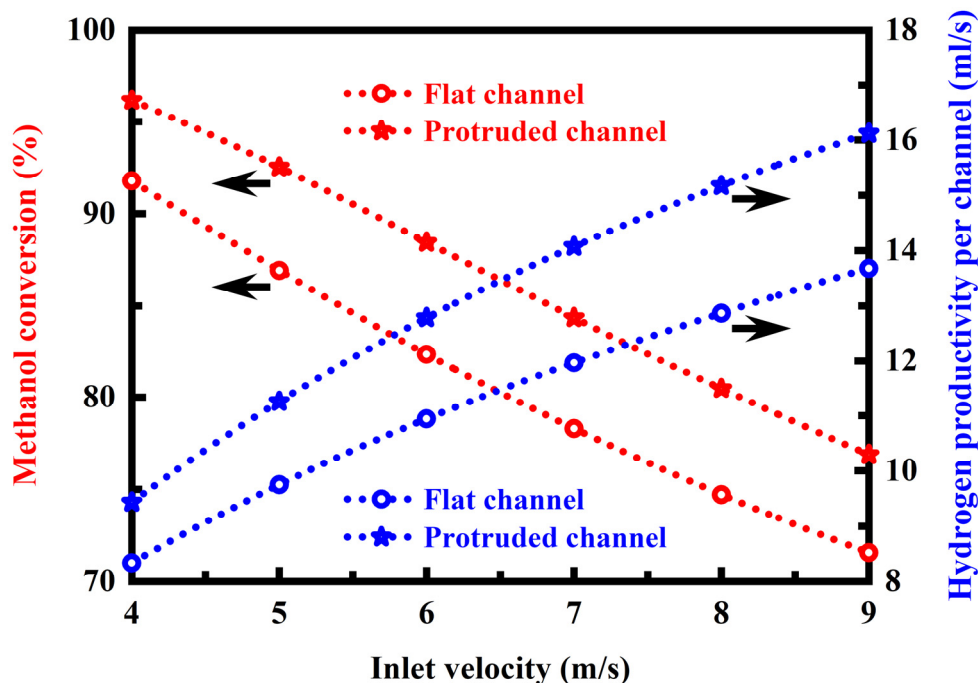

Figure 7. Effects of the velocity at the reactor inlet on the methanol conversion and the hydrogen productivity per channel.

In comparison to Reynolds number, the Prandtl number is not dependent on geometry of an object involved in the problem, but is dependent solely on the fluid and the fluid state. As such, the Prandtl number is often found in property tables alongside other properties such as viscosity and thermal conductivity. One of the main challenges in numerical simulation is the reliable modelling of heat transfer in the reactor by computational fluid dynamics. Heat transfer applications with low-Prandtl number fluids are often in the transition range between conduction and convection dominated regimes. In the special case where the Prandtl number and turbulent Prandtl number both equal to unity, as in the Reynolds analogy, the velocity profile and temperature profiles are identical. This greatly simplifies the solution of the heat transfer problem.

The effect of the velocity at the reactor inlet on the Prandtl number of the gas mixture is illustrated in Figure 8 in which the Prandtl number is averaged over the solution domain. The fluid domain associated with the model, in which the fluid flows in or out the channel, has a Prandtl number higher than the porous domain, which means that the thermal diffusivity is more dominant in the porous domain than in the fluid domain. At lower inlet velocities, the thickness of thermal boundary layer in laminar flow is greater than the that of velocity boundary layer, since the Prandtl number is less than unity. As the inlet velocity increases, the Prandtl number in the fluid domain tends to unity. In such a situation, momentum and thermal diffusion coefficients are comparable and the velocity and thermal boundary layers coincide with each other. The Prandtl number increases with the velocity at the reactor inlet, which means that the momentum diffusivity is more dominant at higher inlet velocities than at lower inlet velocities. While the Prandtl number in the fluid region is sensitive to the velocity at the reactor inlet, the Prandtl number in the porous region does not vary substantially. The Prandtl number

over the total solution domain increases with the velocity at the reactor inlet but is still less than unity, which means that the thermal diffusivity dominates the overall reactor behaviour.
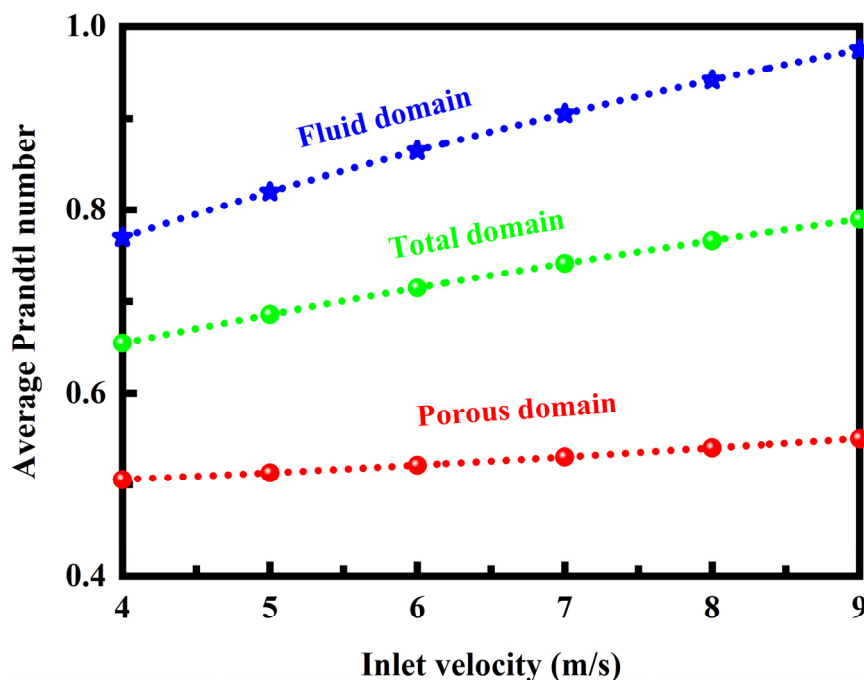

Figure 8. Effect of the velocity at the reactor inlet on the Prandtl number of the gas mixture averaged over the solution domain.

4. Conclusions

Numerical modelling for the design of a millisecond microchannel reforming reactor was conducted using computational fluid dynamics in order to delineate the role of geometric features and operation conditions in reactor performance. The reforming channels are designed in a protruded manner. The effects of inlet velocity, steam-to-methanol ratio, equivalence ratio, and channel length were investigated understand how to improve the efficiency and performance of the reactor. Dimensionless Prandtl numbers are used to facilitate analysis of the transport processes involved.

The conclusions are summarized primarily as follows: Process intensification is realized due primarily to the generation of wake vortices behind the protrusions with increased contact times. The momentum diffusivity is more dominant around the protrusion regions than in the other regions. The thermal diffusivity is more dominant in the protruded channels than in the flat channels. The flow rates must be closely adjusted to satisfy the reaction conditions in practice, thereby ensuring efficient operation of the reactor, such as improved hydrogen production and reduced pressure drops. Protrusions are very effective in improving the transport processes involved without greatly impairing hydraulic performance, and high conversions and good yields can be obtained with only milliseconds residence of the mixtures within the reactor. The protruded design enables a higher conversion level and improved hydrogen productivity in the chemical process by virtue of improved species transport from and to the washcoat coating surface.

References

[1] H. Pennemann, P. Watts, S.J. Haswell, V. Hessel, and H. Löwe. Benchmarking of microreactor applications. *Organic Process Research & Development*, Volume 8, Issue 3, 2004, Pages 422-439.
[2] J. Zong and J. Yue. Continuous solid particle flow in microreactors for efficient chemical conversion. *Industrial & Engineering Chemistry Research*, Volume 61, Issue 19, 2022, Pages

6269-6291.

[3] O. Wörz, K.P. Jäckel, T. Richter, and A. Wolf. Microreactors, a new efficient tool for optimum reactor design. *Chemical Engineering Science*, Volume 56, Issue 3, 2001, Pages 1029-1033.

[4] H. Kestenbaum, A.L. de Oliveira, W. Schmidt, F. Schüth, W. Ehrfeld, K. Gebauer, H. Löwe, and T. Richter. Synthesis of ethylene oxide in a catalytic microreactor system. *Studies in Surface Science and Catalysis*, Volume 130, 2000, Pages 2741-2746.

[5] P. Claus, D. Hönicke, and T. Zech. Miniaturization of screening devices for the combinatorial development of heterogeneous catalysts. *Catalysis Today*, Volume 67, Issue 4, 2001, Pages 319-339.

[6] Z. Dong, Z. Wen, F. Zhao, S. Kuhn, and T. Noël. Scale-up of micro- and milli-reactors: An overview of strategies, design principles and applications. *Chemical Engineering Science: X*, Volume 10, 2021, Article Number: 100097.

[7] D.C. Walther and J. Ahn. Advances and challenges in the development of power-generation systems at small scales. *Progress in Energy and Combustion Science*, Volume 37, Issue 5, 2011, Pages 583-610.

[8] J.D. Holladay and Y. Wang. A review of recent advances in numerical simulations of microscale fuel processor for hydrogen production. *Journal of Power Sources*, Volume 282, 2015, Pages 602-621.

[9] A. Kraytsberg and Y. Ein-Eli. Review of advanced materials for proton exchange membrane fuel cells. *Energy & Fuels*, Volume 28, Issue 12, 2014, Pages 7303-7330.

[10] G. Zhang, Z. Qu, W.-Q. Tao, X. Wang, L. Wu, S. Wu, X. Xie, C. Tongsh, W. Huo, Z. Bao, K. Jiao, and Y. Wang. Porous flow field for next-generation proton exchange membrane fuel cells: materials, characterization, design, and challenges. *Chemical Reviews*, Volume 123, Issue 3, 2023, Pages 989-1039.

[11] N. Marx, L. Boulon, F. Gustin, D. Hissel, and K. Agbossou. A review of multi-stack and modular fuel cell systems: Interests, application areas and on-going research activities. *International Journal of Hydrogen Energy*, Volume 39, Issue 23, 2014, Pages 12101-12111.

[12] A. Kampker, H. Heimes, M. Kehrer, S. Hagedorn, P. Reims, and O. Kaul. Fuel cell system production cost modeling and analysis. *Energy Reports*, Volume 9, Supplement 1, 2023, Pages 248-255.

[13] J. Min, S.S. Chougule, B. Sravani, K. Ko, Y. Kim, and N. Jung. A bottom-up approach to solving technical challenges in fuel cell systems through innovative catalyst design. *Current Opinion in Electrochemistry*, Volume 39, 2023, Article Number: 101257.

[14] Y. Wang, X. Yang, Z. Sun, and Z. Chen. A systematic review of system modeling and control strategy of proton exchange membrane fuel cell. *Energy Reviews*, Volume 3, Issue 1, 2024, Article Number: 100054.

[15] R.K. Ahluwalia, X. Wang, J. Kwon, A. Rousseau, J. Kalinoski, B. James, and J. Marcinkoski. Performance and cost of automotive fuel cell systems with ultra-low platinum loadings. *Journal of Power Sources*, Volume 196, Issue 10, 2011, Pages 4619-4630.

[16] Y. Sun, M. Delucchi, and J. Ogden. The impact of widespread deployment of fuel cell vehicles on platinum demand and price. *International Journal of Hydrogen Energy*, Volume 36, Issue 17, 2011, Pages 11116-11127.

[17] J. Yampolsky and C.F. Price. Closed-vessel hydrogen-air explosions at high pressures. *Symposium (International) on Combustion*, Volume 4, Issue 1, 1953, Pages 384-386.

[18] R.C. Aiken. A criterion for the isothermal first explosion limit. *Combustion and Flame*, Volume 47, 1982, Pages 281-289.

[19] H.S. Rad, S.M. Mousavi, and A. Sarmadian. Comparative study on the thermal-hydraulic

performance of tubes enhanced with three different types of teardrop protrusions. *Applied Thermal Engineering*, Volume 236, Part C, 2024, Article Number: 121682.

[20] J. Joshi and S.K. Sahu. Effect of single and multiple protrusions on thermal performance of slot jet impingement with curved surface. *Applied Thermal Engineering*, Volume 230, Part B, 2023, Article Number: 120757.

[21] R. Zakeri and A. Fazeli. CFD modeling of hydrogen production from glycerol steam reforming in Tesla microchannel reactor. *Fuel*, Volume 357, Part C, 2024, Article Number: 129646.

[22] A. Delparish, S. Koc, B.S. Caglayan, and A.K. Avci. Oxidative steam reforming of glycerol to synthesis gas in a microchannel reactor. *Catalysis Today*, Volume 323, 2019, Pages 200-208.

[23] T.L. Reitz, S. Ahmed, M. Krumpelt, R. Kumar, and H.H. Kung. Characterization of CuO/ZnO under oxidizing conditions for the oxidative methanol reforming reaction. *Journal of Molecular Catalysis A: Chemical*, Volume 162, Issues 1-2, 2000, Pages 275-285.

[24] J.R. Lattner and M.P. Harold. Autothermal reforming of methanol: Experiments and modeling. *Catalysis Today*, Volume 120, Issue 1, 2007, Pages 78-89.

[25] B.A. Peppley, J.C. Amphlett, L.M. Kearns, and R.F. Mann. Methanol-steam reforming on $Cu/ZnO/Al_2O_3$ catalysts. Part 1: The reaction network. *Applied Catalysis A: General*, Volume 179, Issues 1-2, 1999, Pages 21-29.

[26] B.A. Peppley, J.C. Amphlett, L.M. Kearns, and R.F. Mann. Methanol-steam reforming on $Cu/ZnO/Al_2O_3$ catalysts. Part 2. A comprehensive kinetic model. *Applied Catalysis A: General*, Volume 179, Issues 1-2, 1999, Pages 31-49.

[27] D.J. Tritton. Experiments on the flow past a circular cylinder at low Reynolds numbers. *Journal of Fluid Mechanics*, Volume 6, Issue 4, 1959, Pages 547-567.

[28] C.P. Jackson. A finite-element study of the onset of vortex shedding in flow past variously shaped bodies. *Journal of Fluid Mechanics*, Volume 182, 1987, Pages 23-45.

[29] R. López-Ruiz and Y. Pomeau. Transition between two oscillation modes. *Physical Review E*, Volume 55, Issue 4, 1997, Article Number: R3820(R).

[30] S. Piedra, E. Ramos, and J.R. Herrera. Dynamics of two-dimensional bubbles. *Physical Review E*, Volume 91, Issue 6, 2015, Article Number: 063013.

[31] Y. Hu, R.E. Ecke, and G. Ahlers. Behavior of focus patterns in low Prandtl number convection. *Physical Review Letters*, Volume 72, Issue 14, 1994, Pages 2191-2194.

[32] J. Schumacher, V. Bandaru, A. Pandey, and J.D. Scheel. Transitional boundary layers in low-Prandtl-number convection. *Physical Review Fluids*, Volume 1, Issue 8, 2016, Article Number: 084402.

[33] H. Kalman and R. Letan. Thickness of thermal and velocity boundary layers on a mobile surface of a sphere. *International Communications in Heat and Mass Transfer*, Volume 12, Issue 2, 1985, Pages 201-208.

[34] A.J. White. Numerical investigation of condensing steam flow in boundary layers. *International Journal of Heat and Fluid Flow*, Volume 21, Issue 6, 2000, Pages 727-734.

[35] D. Biles, A. Ebadi, M.P. Allard, and C.M. White. The design and validation of a thermal boundary layer wall plate. *Journal of Fluids Engineering*, Volume 141, Issue 12, 2019, Article Number: 121403.

[36] R.J. Butler and J.W. Baughn. The effect of the thermal boundary condition on transient method heat transfer measurements on a flat plate with a laminar boundary layer. *ASME Journal of Heat and Mass Transfer*, Volume 118, Issue 4, 1996, Pages 831-837.

[37] T. Gerz, F. Holzäpfel, and D. Darracq. Commercial aircraft wake vortices. *Progress in Aerospace Sciences*, Volume 38, Issue 3, 2002, Pages 181-208.

[38] J. Ruhland, F.M. Heckmeier, and C. Breitsamter. Experimental and numerical analysis of wake

vortex evolution behind transport aircraft with oscillating flaps. *Aerospace Science and Technology*, Volume 119, 2021, Article Number: 107163.

[39] W. Gerlinger, K. Schneider, L. Falk, and H. Bockhorn. Numerical simulation of the mixing of passive and reactive scalars in two-dimensional flows dominated by coherent vortices. *Chemical Engineering Science*, Volume 55, Issue 19, 2000, Pages 4255-4269.

[40] B.D. Storey and A.M. Jacobi. The effect of streamwise vortices on the frost growth rate in developing laminar channel flows. *International Journal of Heat and Mass Transfer*, Volume 42, Issue 20, 1999, Pages 3787-3802.

[41] J. Wu, J. Sheridan, K. Hourigan, and J. Soria. Shear layer vortices and longitudinal vortices in the near wake of a circular cylinder. *Experimental Thermal and Fluid Science*, Volume 12, Issue 2, 1996, Pages 169-174.

[42] E.K.W. Poon, A.S.H. Ooi, M. Giacobello, and R.C.Z. Cohen. Hydrodynamic forces on a rotating sphere. *International Journal of Heat and Fluid Flow*, Volume 42, 2013, Pages 278-288.

[43] G. Biswas, K. Torii, D. Fujii, and K. Nishino. Numerical and experimental determination of flow structure and heat transfer effects of longitudinal vortices in a channel flow. *International Journal of Heat and Mass Transfer*, Volume 39, Issue 16, 1996, Pages 3441-3451.

[44] J. Mi and R.A. Antonia. Temperature distribution within vortices in the wake of a cylinder. *International Journal of Heat and Mass Transfer*, Volume 37, Issue 6, 1994, Pages 1048-1050.

[45] M. Nurdin. Assessment of strategic approaches to the commercialization of fuel cells. *Journal of Power Sources*, Volume 61, Issues 1-2, 1996, Pages 15-20.

[46] J.M. King and M.J. O'Day. Applying fuel cell experience to sustainable power products. *Journal of Power Sources*, Volume 86, Issues 1-2, 2000, Pages 16-22.

[47] W. Smith. The role of fuel cells in energy storage. *Journal of Power Sources*, Volume 86, Issues 1-2, 2000, Pages 74-83.

[48] C.A. Ward and J.A. Garcia. Analytical method for determining the internal resistance and electrocatalyst utilization of fuel cells. *Journal of Power Sources*, Volume 66, Issues 1-2, 1997, Pages 83-88.